Quantitative J Correlation: A New Approach for Measuring Homonuclear Three-Bond $J(H^NH^\alpha)$ Coupling Constants in ^{15}N-Enriched Proteins

Geerten W. Vuister and Ad Bax*

Contribution from the Laboratory of Chemical Physics, National Institute of Diabetes and Digestive and Kidney Diseases, National Institutes of Health, Bethesda, Maryland 20892

Received April 21, 1993

Abstract: A new approach is described for the measurement of homonuclear H^N–H^α J couplings in ^{15}N-enriched proteins. The method relies on measurement of the diagonal-peak to cross-peak intensity ratio in a 3D ^{15}N-separated quantitative J-correlation spectrum. The experiment is demonstrated for the protein staphylococcal nuclease, uniformly enriched with ^{15}N, ligated with thymidine 3′-5′-bisphosphate and Ca^{2+}. Amide to $C^\alpha H$ correlations are observed for all but three of the amide protons that have regular intensities in a 2D ^1H–^{15}N correlation spectrum, and J couplings could be measured for 96 residues with sufficiently resolved ^1H–^{15}N correlations, including 6 glycines. In addition, for 28 residues with partially overlapping ^1H–^{15}N correlations, coupling constants can be estimated as small, medium, or large. For 86 out of the 96 residues, the backbone angle ϕ is known with good precision from the crystal structure, and J values for these residues have a 0.73 Hz root-mean-square deviation from the Karplus curve: $J = A\cos^2(\phi - 60) + B\cos(\phi - 60) + C$, where $A = 6.51$, $B = -1.76$, $C = 1.60$.

The homonuclear three-bond $J(H^NH^\alpha)$ coupling constant contains valuable information regarding the intervening dihedral backbone angle ϕ in peptides and proteins. The magnitude of the $J(H^NH^\alpha)$ coupling can be related to this angle by using the well-known Karplus equation,[1,2] which has been parametrized for this purpose by using low molecular weight compounds of accurately known geometry[2-5] or by correlating the J values measured in small globular proteins with dihedral angles obtained from crystallographic studies.[6,7] Accurate measurement of homonuclear J couplings in proteins is fraught with problems that are related to the small size of these couplings relative to the natural proton line width. In particular for proteins larger than about 10 kD, quantitative measurement of homonuclear J couplings can be problematic. To date, a variety of methods have been introduced for measurement of H^N–H^α J couplings. These include various fitting procedures used for the measurement of antiphase doublet splittings in COSY-type spectra,[7-9] ECOSY-type triple resonance experiments on proteins uniformly enriched with both ^{13}C and ^{15}N,[10-12] measurement of the splitting in resolution-enhanced ^{15}N–^1H HMQC spectra,[13,14] nonlinear fitting of J-modulated ^{15}N–^1H HSQC spectra,[15] and fitting of in-phase splittings in 2D spectra.[16] Although some of these methods are more robust than others for measuring accurate J values in proteins larger than ~10 kD, all but the $^{15}N/^{13}C$-based ECOSY techniques decrease in accuracy when the line width becomes significantly larger than the J coupling. This frequently presents a problem for the measurement of small J couplings, such as typically encountered in α-helical regions of a protein ($J(H^NH^\alpha)$ ~ 4 Hz). The ECOSY type experiments do not require the coupling to be resolved, but the accuracy with which J values can be measured is limited by the precision with which peak positions can be determined in 3D NMR spectra. In all these experiments, the value of the measured J coupling is also influenced by the rate of ^1H–^1H spin diffusion.[17] Here we describe a different approach for measurement of the $J(H^NH^\alpha)$ coupling, which in many respects is advantageous over the methods mentioned above. The method relies on quantitative analysis of the diagonal-peak to cross-peak intensity ratio in a ^{15}N-separated H^N–H^α homonuclear J correlation experiment. This experiment has been designed in such a way that this ratio, to a first approximation, is independent of the transverse relaxation rates of the H^N and H^α resonances involved. The approach is conceptually similar to the one recently used for measurement of long-range homonuclear ^{13}C–^{13}C J couplings[18] and heteronuclear ^1H–^{113}Cd and ^1H–^{199}Hg couplings in proteins.[19] In addition to the value of $J(H^NH^\alpha)$, the new scheme also provides the intraresidue $J(H^NH^\alpha)$ correlation information, which makes it a useful alternative to other methods used for this purpose.[10,20-23] In analogy with the nomenclature developed for related triple-resonance experiments,[24] we propose to name this experiment HNHA as it correlates the intraresidue $^1H^N$, ^{15}N, and $^1H^\alpha$ resonances.

(1) Karplus, M. *J. Chem. Phys.* **1959**, *30*, 11–15.
(2) Bystrov, V. F. *Prog. NMR. Spectrosc.* **1976**, *10*, 41–81.
(3) Bystrov, V. F.; Portnova, S. L.; Tsetlin, V. I.; Ivanov, V. I.; Ovchinnikov, Y. A. *Tetrahedron* **1969**, *25*, 493–515.
(4) Feeney, J. *Proc. R. Soc. London, Ser. A* **1975**, *345*, 61–72.
(5) DeMarco, A.; Llinas, M.; Wüthrich, K. *Biopolymers* **1978**, *17*, 647–650.
(6) Pardi, A.; Billeter, M.; Wüthrich, K. *J. Mol. Biol.* **1984**, *180*, 741–751.
(7) Ludvigsen, S.; Andersen, K. V.; Poulsen, F. M. *J. Mol. Biol.* **1991**, *217*, 731–736.
(8) Smith, L. J.; Sutcliffe, M. J.; Redfield, C.; Dobson, C. M. *Biochemistry* **1991**, *30*, 986–996.
(9) Neuhaus, D.; Wagner, G.; Vasak, M.; Kägi, J. H. R.; Wüthrich, K. *Eur. J. Biochem.* **1985**, *151*, 257–273.
(10) Montelione, G. T.; Wagner, G. *J. Am. Chem. Soc.* **1989**, *111*, 5474–5475.
(11) Wagner, G.; Schmieder, P.; Thanabal, V. *J. Magn. Reson.* **1991**, *93*, 436–440.
(12) Schmieder, P.; Thanabal, V.; McIntosh, L. P.; Dahlquist, F. W.; Wagner, G. *J. Am. Chem. Soc.* **1991**, *113*, 6323–6324.
(13) Kay, L. E.; Brooks, B.; Sparks, S. W.; Torchia, D. A.; Bax, A. *J. Am. Chem. Soc.* **1989**, *111*, 5488–5490.
(14) Kay, L. E.; Bax, A. *J. Magn. Reson.* **1989**, *86*, 110–126.
(15) Billeter, M.; Neri, D.; Otting, G.; Qian, Y. Q.; Wüthrich, K. *J. Biomol. NMR* **1992**, *2*, 257–274.
(16) Szyperski, T.; Güntert, P.; Otting, G.; Wüthrich, K. *J. Magn. Reson.* **1992**, *99*, 552–560.
(17) Harbison, G. *J. Am. Chem. Soc.* **1993**, *115*, 3026–3027.
(18) Bax, A.; Max, D.; Zax, D. *J. Am. Chem. Soc.* **1992**, *114*, 6924–6925.
(19) Blake, P. R.; Summers, M. F.; Adams, M. W. W.; Park, J.-B.; Zhou, Z. H.; Bax, A. *J. Biomol. NMR* **1992**, *2*, 527–533.
(20) Marion, D.; Driscoll, P. C.; Kay, L. E.; Wingfield, P. T.; Bax, A.; Gronenborn, A. M.; Clore, G. M. *Biochemistry* **1989**, *28*, 6150–6156.
(21) Kay, L. E.; Ikura, M.; Bax, A. *J. Magn. Reson.* **1991**, *91*, 84–92.
(22) Clubb, R. T.; Thanabal, V.; Wagner, G. *J. Biomol. NMR* **1992**, *2*, 203–210.
(23) Seip, S.; Balbach, J.; Kessler, H. *J. Magn. Reson.* **1992**, *100*, 406–410.
(24) Ikura, M.; Kay, L. E.; Bax, A. *Biochemistry* **1990**, *29*, 4659–4667.

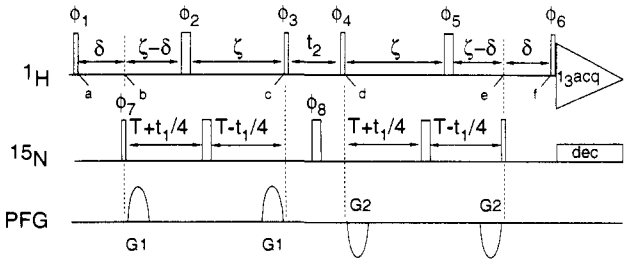

Figure 1. Pulse scheme of the 3D HNHA experiment. Narrow and wide pulses denote 90° and 180° flip angles, respectively. Unless indicated otherwise, all pulses are applied along the x-axis. For the version using pulsed field gradients (PFG) the following phase cycle is used: $\phi_1 = x$; $\phi_2 = 4x,4(-x)$; $\phi_3 = x,-x$; $\phi_4 = 2x,2(-x)$; $\phi_5 = 4x,4(-x)$; $\phi_6 = y,-y$; $\phi_7 = x$; $\phi_8 = 8x,8y$; receiver = $8x, 8(-x)$. Pulsed field gradients are not essential, and for the version without PFGs the following 32-step phase cycle can be used: $\phi_1 = x$; $\phi_2 = 4x,4(-x),4(y),4(-y)$; $\phi_3 = x,-x$; $\phi_4 = 2x,2(-x)$; $\phi_5 = 4x,4y,4(-x),4(-y)$; $\phi_6 = y,-y$; $\phi_7 = x$; $\phi_8 = 16x,16y$; receiver = $4x,8(-x),4x,4(-x),8x,4(-x)$. Quadrature detection in t_1 and t_2 is obtained with the States-TPPI method, incrementing phases ϕ_7 for t_1 and ϕ_1, ϕ_2, and ϕ_3 for t_2. Pulsed field gradients have a sine-bell shape with a strength of 10 G/cm at their maximum and are applied along the z-axis. PFG durations are $G_1 = 750\,\mu s$ and $G_2 = 750\,\mu s$ (negative polarity). The delay δ is set to 4.5 ms and the delay ζ is set to 13.05 ms. Solvent suppression was achieved by irradiation with a weak RF field ($\gamma B_2 2\pi \sim 25$ Hz) during the relaxation delay. ^{15}N decoupling during data acquisition was accomplished with use of an asynchronous WALTZ-16 decoupling scheme[46] with an RF field strength of 1.6 kHz.

The HNHA experiment is demonstrated for the protein staphylococcal nuclease (SNase). Precise coupling constants could be measured for 96 residues with non-overlapping ^{15}N–H^N correlations and that were not attenuated by either exchange with solvent or slow conformational averaging. For 84 of these residues, the backbone angle ϕ is known with good precision from crystallographic studies.[25] Least-squares fitting of the measured J couplings to a Karplus equation, $J = A\cos^2(\phi - 60) + B\cos(\phi - 60) + C$, and optimal parametrization of this equation will be discussed. Compared to an earlier measurement of $J(H^NH^\alpha)$ couplings in SNase,[13] the present study allows measurement of a significantly larger number of couplings, particularly for residues with J values smaller than 5 Hz.

Experimental Section

The experiment was performed on a sample containing 1.5 mM SNase, uniformly (>95%) enriched with ^{15}N, in the presence of 100 mM NaCl, 5 mM thymidine 3′-5′-bisphosphate, and 10 mM $CaCl_2$. The sample was dissolved in 95% H_2O/5% D_2O, pH 7.0. Expression and purification of the protein have been described previously,[26] and resonance assignments as reported by Baldisseri *et al.*[27] were used. The experiment was carried out at 35 °C on a Bruker AMX600, operating at a ^1H resonance frequency of 600.13 MHz, and equipped with a Bruker triple-resonance probe with a self-shielded z-gradient. Pulsed field gradients were generated with an in-house developed gradient pulse-shaping unit and amplifier. Sine-bell shaped gradient pulses had a strength of 10 G/cm at the center of the sine-bell. The HNHA spectrum was recorded with the pulse scheme of Figure 1, as a $48^*(t_1) \times 48^*(t_2) \times 512^*(t_3)$ data set, were n^* denotes n complex data points, with acquisition times of 39.17, 10.56, and 42.00 ms, respectively. The total measuring time, using 64 scans for each pair of t_1/t_2 values, was 45 h. The data were processed using in-house written routines for all dimensions. In the t_3 dimension a solvent-suppression filter was applied to the time domain data[28] before apodization with a 66° shifted squared sine-bell window, zero-filling to 1024*, Fourier transformation, phasing, and discarding of the upfield half of the spectrum. The data were apodized in t_2 by a 72° shifted sine-bell window prior to zero-filling to 256*, Fourier transformation, and phasing. Finally, the duration of the nondecaying t_1 time-domain data was doubled by mirror-image linear prediction,[29] apodized by a squared cosine-bell window, zero filled to 128*, and Fourier transformed. The size of the absorptive part of the resulting 3D spectrum was $128(F_1) \times 256(F_2) \times 512(F_3)$. Small baseline distortions in F_3 were removed by an automatic third-order polynomial baseline correction routine.

Peak positions and intensities for non-overlapping peaks were located interactively by using 3D parabolic interpolation as implemented in the program PIPP.[30] For resonances subject to partial overlap, a 3D spectral simulation and deconvolution procedure was used correcting peak intensities for the contributions of the tails of neighboring peaks.[31]

A simple least-squares minimization routine based on singular-value-decomposition was used to determine the A, B, and C parameters of the Karplus equation (*cf.* eq 5) that yield the best fit between the measured J values and the known backbone angles ϕ. In this process, 86 residues with crystallographically well-defined backbone angles ϕ were used, including five glycines. Stereospecific assignments for pro-chiral H^α atoms of glycine residues were obtained by comparison of NOE patterns observed in a 4D ^{13}C-separated NOESY spectrum with the NOE patterns expected on the basis of the crystal structure.[25]

Results and Discussion

Description of the Pulse Scheme. The pulse scheme used in the present work is shown in Figure 1, and will be briefly discussed below. A more complete description of the pulse sequence, using the product operator formalism, is presented in the supplementary material. For the present discussion it is sufficient to consider a simple system comprised of the proton amide spin (H^N), the H^α spin, coupled to H^N with coupling constant $^3J(H^NH^\alpha)$ (denoted by J_{HH}), and the ^{15}N spin, coupled to H^N with a coupling constant $^1J(NH)$. Proton magnetization, generated by the first $90°_{\phi_1}$ ^1H pulse, and present at time a in Figure 1, dephases with respect to its attached ^{15}N spin during the delay δ. Zero- and double-quantum terms are generated by the $90°_{\phi_7}(^{15}N)$ pulse applied at time b, in an HMQC type fashion.[32,33] Simultaneous displacement of the first and third 180° ^{15}N pulses during the subsequent delays, of total duration $4T + t_2$, causes chemical shift labeling of the ^{15}N spin in a constant-time manner.[34,35] Signals are not modulated by $^1J(NH)$ because evolution of the zero- and double-quantum terms is not affected by the one-bond J coupling between the H^N and ^{15}N spins.

Between time points a and c dephasing occurs as a result of the homonuclear H^N–H^α J coupling, active for a total duration of 2ζ. As a result, terms develop that contain amide proton magnetization which is antiphase with respect to the H^α spin and are proportional to $\sin(2\pi J_{HH}\zeta)$.

The amide antiphase term is converted in antiphase H^α magnetization by the $90°_{\phi_3}$ ^1H pulse. After the short t_2 evolution period, antiphase H^α magnetization terms are converted back to antiphase amide magnetization. During the subsequent rephasing period, between time points d and f, homonuclear H^N–H^α J coupling is active again, and rephasing proportional to $\sin(2\pi J_{HH}\zeta)$ occurs. The $90°(^{15}N)$ pulse applied at time e converts multiple quantum terms back into H^N magnetization that is antiphase with respect to its attached ^{15}N spin. This antiphase magnetization subsequently rephases during the second delay δ. After the $90°_{\phi_6}$ purge pulse, only amide proton magnetization that originates from in-phase terms is observed during t_3. The observed signal $S(t_1,t_2,t_3)$ is purely absorptive and described by

(25) Loll, P. J.; Lattman, E. E. *Proteins: Struct., Funct., Genet.* **1989**, *5*, 183–201.
(26) Torchia, D. A.; Sparks, S. W.; Bax, A. *Biochemistry* **1989**, *28*, 5509–5524.
(27) Baldisseri, D. M.; Torchia, D. A. Poole, L. B.; Gerlt, J. *Biochemistry* **1991**, *30*, 3628–3633.
(28) Marion, D.; Ikura, M.; Bax, A. *J. Magn. Reson.* **1989**, *84*, 425–430.
(29) Zhu, G.; Bax, A. *J. Magn. Reson.* **1990**, *90*, 405–410.
(30) Garrett, D. S.; Powers, R.; Gronenborn, A. M.; Clore, G. M. *J. Magn. Reson.* **1991**, *95*, 214–220.
(31) Delaglio, F., unpublished results.
(32) Mueller, L. *J. Am. Chem. Soc.* **1979**, *101*, 4481–4484.
(33) Bax, A.; Griffey, R. H.; Hawkins, B. L. *J. Magn. Reson.* **1983**, *55*, 301–315.
(34) Sørensen, O. W. *J. Magn. Reson.* **1990**, *90*, 433–438.
(35) Powers, R.; Gronenborn, A. M.; Clore, G. M.; Bax, A. *J. Magn. Reson.* **1991**, *94*, 209–213.

$$S(t_1,t_2,t_3) = A\{\cos^2(2\pi J_{HH}\zeta)\cos(\omega_N t_1)\cos(\omega_{HN} t_2) - \sin^2(2\pi J_{HH}\zeta)\cos(\omega_N t_1)\cos(\omega_\alpha t_2)\}\exp(i\omega_{HN} t_3) \quad (1)$$

where ω_{HN}, ω_N, and ω_α are the angular offset frequencies of the amide proton, amide nitrogen, and H^α proton, respectively. The constant A includes trigonometric functions of the one-bond heteronuclear nitrogen-proton coupling J(NH) (~92 Hz) and the heteronuclear ^{15}N–H^α coupling $J(NH^\alpha)$, active during parts of the pulse sequence (see supplementary material).

In the F_1 and F_3 dimensions, the line shape of the "diagonal peak" at $(F_1,F_2,F_3) = (\omega_N,\omega_{HN},\omega_{HN})$ and the cross peak at $(F_1,F_2,F_3) = (\omega_N,\omega_\alpha,\omega_{HN})$ is determined by identical factors. In the F_2 dimension, the intrinsic line widths of the diagonal and cross peaks are determined by the decay rates of transverse H^N and H^α magnetization during t_2. However, in the present experiment the acquisition time in the t_2 dimension is much shorter than the transverse relaxation time of either H^N or H^α. As a result, the line shape in the F_2 dimension is determined primarily by the apodization function used in the t_2 dimension. Therefore, diagonal and cross peaks also have identical line shapes in the F_2 dimension and the intensity ratio S_{cross}/S_{diag} then provides a direct measure for the magnitude of J_{HH}:

$$S_{cross}/S_{diag} = -\tan^2(2\pi J_{HH}\zeta) \quad (2)$$

Because of the simplicity of the relationship between the diagonal and cross-peak intensities in the purged version of the experiment, this is the method of choice for measuring J couplings quantitatively. However, if the main purpose is to establish J connectivities in a qualitative way, removal of the $90°_{\phi_6}$ purge pulse generally will yield higher signal-to-noise ratios because the observed magnetization, originating from antiphase terms at time f in the pulse scheme, continues to rephase during the detection period, t_3 (*cf.* eq 8a,b of the supplementary material).

The pulsed-field gradients (PFG) sketched in Figure 1 are not essential for the experiment. They merely serve to reduce the artifacts associated with pulse imperfections and thereby permit a reduction of the phase cycle. The phase cycles for both versions of the experiment are given in the legend to Figure 1.

Experimental Results. The HNHA experiment offers excellent sensitivity in spite of the long dephasing and rephasing delays 2ζ. As an example of the obtained spectral quality, Figure 2 shows seven F_2 strips from the HNHA spectrum of SNase, taken at the ^{15}N–^1H resonance frequencies of residues Tyr85-Tyr91. The F_2 region between 7.0 and 9.5 ppm contains the "diagonal" peaks, which correspond to magnetization not transferred to H^α during t_2. The cross peaks between amides and H^α resonances are located in the F_2 region between 3.5 and 5.5 ppm. Due to the 3D nature of the experiment and the high resolution obtainable in the constant-time ^{15}N dimension, cross peaks are virtually free of overlap. Of course, overlap of the "diagonal" resonances is comparable to that in a high-resolution 2D ^1H–^{15}N correlation spectrum.

Precise H^N–H^α J values could be measured for 96 residues in SNase. No couplings could be measured for the 5 N-terminal residues because of fast amide proton exchange with solvent, for 6 prolines, and for 11 residues with very weak or absent ^{15}N–^1H correlations, most of which are located in the conformationally averaged Ω-loop of SNase.[26] For 3 residues, no H^N–H^α connectivity was observed and only an upper limit for the J coupling could be calculated. For 28 residues, only a qualitative estimate of the size of the J coupling could be made because of overlap of the diagonal ^{15}N–H^N correlation.

Measurement of *J* Couplings. Besides establishing intraresidue H^N–H^α J connectivity, the main purpose of the HNHA experiment is to measure the size of the homonuclear $^3J(H^NH^\alpha)$ coupling constants, using eq 2. In deriving eq 2, the implicit assumption is made that during the de- and rephasing delays, 2ζ, the magnetization components giving rise to diagonal and cross peaks

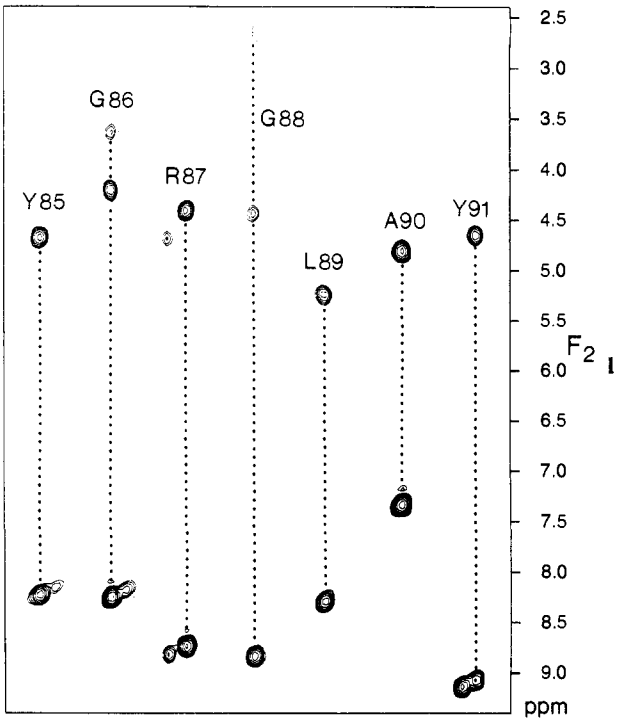

Figure 2. F_2 strips from the 3D HNHA spectrum of SNase, taken at the ^{15}N–^1H resonance positions of Tyr85–Tyr91. Resonances in the F_2 region between 3.5 and 5.5 ppm are H^N–H^α cross peaks with negative intensities and resonances downfield of F_2 = 7 ppm are H^N diagonal peaks with positive intensities. The cross-peak to diagonal-peak intensity ratio presents a measure for the $^3J(H^NH^\alpha)$ coupling.

relax at identical rates. If the amide spin is described by an operator I^N and the H^α spin by I^α, it is well-known that antiphase magnetization of the form $2I^N_xI^\alpha_z$ relaxes at a faster rate than the in-phase component I^N_y.[36-38] For proteins in the slow-motion limit, the relaxation time of the antiphase magnetization (T_{2ap}) to a good approximation is given by:

$$1/T_{2ap} = 1/T_{2HN} + 1/T_{1sel} \quad (3)$$

where T_{2HN} is the transverse relaxation time of the in-phase H^N magnetization and T_{1sel} describes the apparent selective T_1 of the H^α spin. It should be noted that selective inversion recovery of protons in proteins is a non-exponential process, which is determined primarily by cross relaxation with other protons. A good estimate for the apparent value of $1/T_{1sel}$, as needed to correct for the faster relaxation of $2I^N_xI^\alpha_z$ during the period 2ζ, can be derived indirectly from separate experiments which measure the decay of I_zS_z and S_z terms during a period 2ζ. Using this approach, T_{1sel} values of ~100 ms are found for the amide protons in SNase,[39] and values in the 100–200-ms range for the H^α protons of alanine residues in nonflexible parts of [$^{13}C^\alpha$-Ala]-SNase (Nicholson and Torchia, unpublished results). For proteins in the slow tumbling limit, these values scale with the inverse of the protein rotational correlation time τ_c.

Because the H^N–H^α cross peaks and the H^N–H^N diagonal peaks result from the antiphase and in-phase terms, respectively, the faster relaxation of the antiphase $2I^N_xI^\alpha_z$ term attenuates the cross peak relative to the diagonal peak, resulting in an underestimate of the J coupling (*cf.* eq 2). However, as will be discussed below, the fractional error in the derived J coupling, caused by this relaxation effect, is to a good approximation

(36) Bax, A.; Ikura, M.; Kay, L. E.; Torchia, D. A.; Tschudin, R. *J. Magn. Reson.* **1990**, *86*, 304–318.
(37) London, R. E. *J. Magn. Reson.* **1990**, *86*, 410–415.
(38) Peng, J.; Thanabal, V.; Wagner, G. *J. Magn. Reson.* **1991**, *95*, 421–427.
(39) Kay, L. E.; Nicholson; Delaglio, F.; Bax, A.; Torchia, D. A. *J. Magn. Reson.* **1992**, *97*, 359–375.

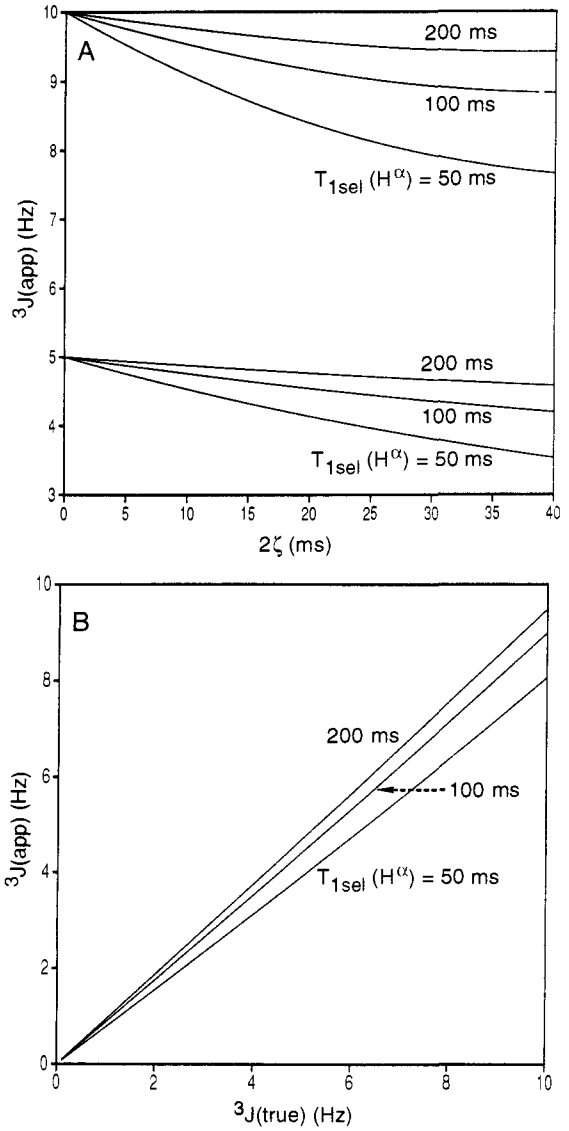

Figure 3. (A) The relation between the apparent H^N–H^α coupling, ^3J(app), and the duration of the de- and rephasing intervals, 2ζ, for three values of $T_{1sel}(H^\alpha)$ and true couplings of 5 and 10 Hz. (B) ^3J(app) *versus* the true coupling, ^3J(true), for three values of $T_{1sel}(H^\alpha)$ and a 2ζ duration of 26.3 ms.

independent of the size of the coupling and can be corrected for in a straightforward way if an estimate for the H^α flip-rate is available.

The time dependence of the in-phase and antiphase amide proton magnetization during the dephasing period, 2ζ, is described by the following differential equations:

$$d\langle I^N_y\rangle/dt = \pi J_{HH}\langle 2I^N_x I^\alpha_z\rangle - \langle I^N_y\rangle/T_{2HN} \quad (4a)$$

$$d\langle 2I^N_x I^\alpha_z\rangle/dt = -\pi J_{HH}\langle I^N_y\rangle - \langle 2I^N_x I^\alpha_z\rangle/T_{2HN} - \langle 2I^N_x I^\alpha_z\rangle/T_{1sel} \quad (4b)$$

where $\langle I^N_y\rangle$ and $\langle 2I^N_x I^\alpha_z\rangle$ are the in-phase and antiphase amide magnetization components, respectively. Using the fact that $\langle I^N_y\rangle = 1$ and $\langle 2I^N_x I^\alpha_z\rangle = 0$, at $t = 0$, the $\langle 2I^N_x I^\alpha_z\rangle/\langle I^N_y\rangle$ ratio at time $t = 2\zeta$ can be derived by numerical integration. The apparent coupling, ^3J(app), calculated from this ratio is plotted in Figure 3A as a function of the dephasing delay 2ζ for three values of the H^α flip rate (T_{1sel}^{-1}) and J_{HH} values of 5 and 10 Hz. As expected, the faster relaxation of antiphase magnetization increases the difference between ^3J(app) and J_{HH} with increasing duration 2ζ. Figure 3B shows the relation between ^3J(app) and J_{HH} for a fixed value of 2ζ (26.3 ms), again for three values of T_{1sel}. As can be seen in Figure 3B, for a given value of T_{1sel} the difference between J_{HH} and ^3J(app) increases approximately linearly with J_{HH}. For a T_{1sel} value of 100 ms, J_{HH} is 11% larger than ^3J(app), allowing a simple correction to be made by multiplying the measured coupling by 1.11. After application of this correction factor, there was no systematic difference between our present measurement of J_{HH} and values measured previously.[13]

For glycine residues, the strong dipolar interaction between the geminal H^α protons gives rise to faster cross relaxation rates, i.e., shorter T_{1sel} values, than for most other residues. In this case, a $H^{\alpha1}$–$H^{\alpha2}$ spin flip converts $2I^N_x I^{\alpha1}_z$ into $2I^N_x I^{\alpha2}_z$ and *vice versa*. This causes a decrease in the value measured for the larger of the two H^N–H^α J couplings and a concomitant increase for the smaller one.[40] Cross relaxation to other protons causes both values to decrease in the manner discussed above for non-glycine residues.

The effect of cross relaxation on the measurement of J_{HH} values in the present HNHA experiment is quite analogous to the effect of spin diffusion on NOE buildup in a NOESY experiment. Therefore, it would also be desirable to measure the buildup of H^N–H^α cross peaks as a function of the dephasing period 2ζ, analogous to what is commonly done for measurement of NOE buildup rates. In practice, however, this is not easily achieved because a shorter duration of 2ζ reduces the intensity of the cross peak relative to the diagonal peak and, since the cross peak intensity is almost always smaller than the diagonal peak, it lowers the precision of the measurement of J. In addition, reducing 2ζ also limits the maximum length of the t_1 acquisition period, resulting in insufficient resolution in the ^{15}N dimension of the 3D spectrum. Fortunately, because the dephasing period, 2ζ, is relatively short compared to the ^1H–^1H cross-relaxation rates, a simple correction based on the average H^α flip rate is adequate in practice.

In the absence of relaxation, the HNHA method for measuring J couplings would be most precise when the cross peak and diagonal peak are of comparable intensity, requiring $2\zeta \approx 1/(4J_{HH})$. In the presence of rapid transverse relaxation ($T_2 \ll 1/J$), the optimum duration of 2ζ shifts to shorter values and sensitivity of the method is optimized by maximizing the cross-peak intensity, i.e., by maximizing $\sin(2\pi J\zeta)\exp(-2\zeta/T_2)$, yielding $2\zeta \approx T_2$. Slightly shorter durations of 2ζ may be used, without significantly sacrificing sensitivity, in order to reduce the effect of the difference in relaxation between I^N_y and $2I^N_x I^\alpha_z$ type terms, discussed above. The lower limit for J couplings which give rise to an observable H^N–H^α correlation increases linearly with $1/T_2$, *i.e.* linearly with the rotational correlation time of the protein. In SNase, for which a correlation time of 9 ns has been reported,[41] J couplings down to *ca.* 3 Hz give rise to measurable cross-peak to diagonal-peak intensity ratios.

For 96 of the backbone amides, the ^{15}N–^1H correlations are sufficiently well-resolved to allow precise measurement of their cross-peak to diagonal-peak intensity ratios. Six of these residues are glycines, resulting in a total of 102 H^N–H^α J couplings. $^3J(H^NH^\alpha)$ coupling constants were calculated using eq 2 and the 11% correction mentioned above (except for the highly mobile N- and C-terminal residues) and are listed in Table 1 of the supplementary material. An estimate of the accuracy of our measurement can be obtained by comparison with $^3J(H^NH^\alpha)$ values previously measured for SNase using a high-resolution HMQC spectrum.[13] Couplings measured with the two methods have a root-mean-square difference of 0.67 ($n = 56$), suggesting an error of *ca.* 0.5 Hz for each of the individual experiments.

For 28 residues the ^{15}N–^1H correlations are insufficiently resolved to permit a precise measurement of $^3J(H^NH^\alpha)$. However,

(40) Vuister, G. W.; Yamazaki, T.; Torchia, D. A.; Bax, A. *J. Biomol. NMR.*, **1993**, *3*, 297–306.
(41) Kay, L. E.; Torchia, D. A.; Bax, A. *Biochemistry* **1989**, *28*, 8972–8979.

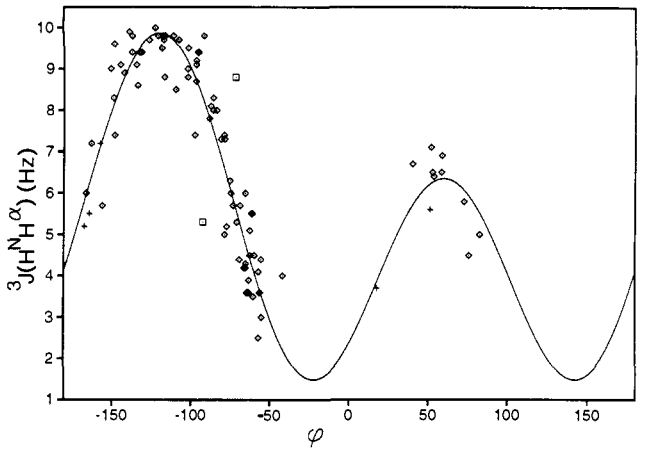

Figure 4. Measured values for 94 $^3J(H^NH^\alpha)$ coupling constants obtained from the HNHA spectrum of the protein SNase, plotted as a function of backbone angle ϕ. $^3J(H^NH^\alpha)$ couplings to the $H^{\alpha 3}$ of glycine residues are indicated by "+". The backbone angle ϕ is offset by 120° for these data points. Lys70 and Lys78 are marked by squares (see text). The solid line indicates the least-squares minimized fit of the Karplus curve (eq 5) with $A = 6.51$, $B = -1.76$, and $C = 1.60$ and a rmsd of 0.73.

for most of these residues a qualitative estimate still can be obtained (supplementary Table I) from the intensities of the cross-peaks, assuming the corresponding diagonal peaks are of average intensity.

For 86 of the residues with precisely determined $^3J(H^NH^\alpha)$ values, including 5 glycines, the backbone angle ϕ is known from previous crystallographic work.[24] Comparing these J values with the values predicted by the Karplus equation

$$J(\phi) = A\cos^2(\phi - 60) + B\cos(\phi - 60) + C \qquad (5)$$

results in a rmsd of 0.76 when the parametrization of Pardi et al.[6] ($A = 6.4$, $B = -1.4$, $C = 1.9$) is used. When the values of Ludvigsen et al.[7] ($A = 6.7$, $B = -1.3$, $C = 1.5$) are used a larger rmsd of 0.82 is obtained. Optimization of the A, B, and C parameters to yield a best fit results in $A = 6.51$, $B = -1.76$, and $C = 1.60$, with a rmsd of 0.73. A plot of the measured values and the best fitted curve is shown in Figure 4. In order to gain insight into the range each of the three parameters can adopt, 12 J values were randomly omitted and a least-squares fitting was performed to obtain optimal A, B, and C values for the remaining 79 J couplings. This procedure was repeated 10 000 times. The resulting distributions of the A, B, and C parameters are shown in Figure 5. Maxima in the three distributions clearly center around the values calculated with use of the complete set ($A = 6.51$, $B = -1.76$, $C = 1.60$). Although the errors in the individual values of ^3J are neither expected to be uncorrelated nor normally distributed, the spread of the A, B, and C parameters observed in Figure 5 correlates well with the calculated variances (0.14, 0.03, and 0.08, respectively).

Both Lys70 and Lys78 deviate significantly (*ca.* +3 and −3 Hz, respectively) from the Karplus curve for any of the three parametrizations. The $J(H^NH^\alpha)$ values measured for these two residues are nearly identical with those measured previously by Kay et al.,[13] and error in the measurement can therefore be excluded. Both these residues are involved in crystal contacts and their ϕ angles are less certain than for most other residues; they changed by +14° and −13° for Lys70 and Lys78, respectively, during the final stage of crystallographic refinement.[42] Because the ϕ angles of Lys70 and Lys78 are near the region where the Karplus equation has its strongest dependence on ϕ, an error of only 25° in ϕ results in a ~3 Hz deviation from the Karplus curve.

(42) Loll, P. J.; Lattman, E. E., personal communication.

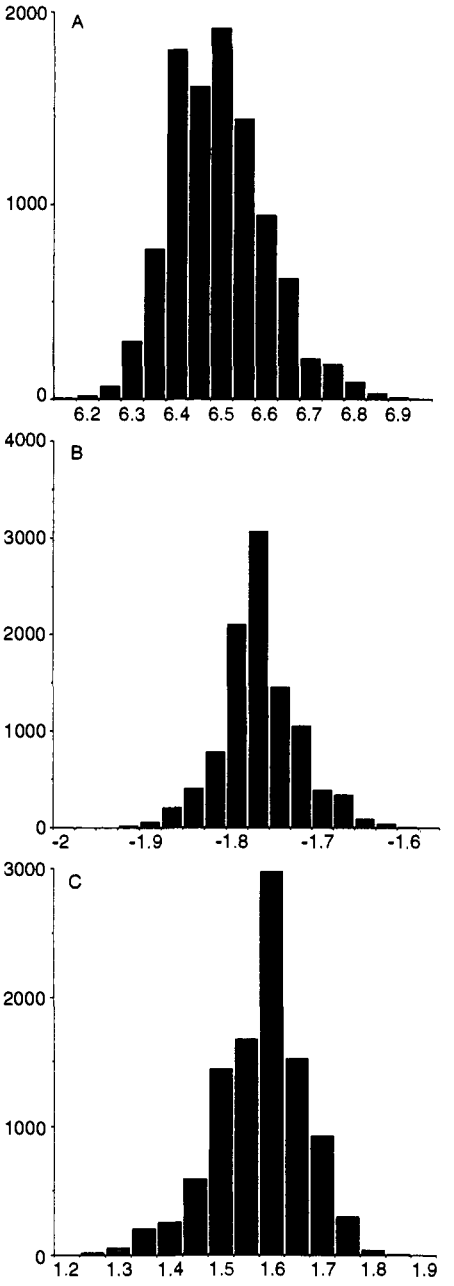

Figure 5. Histograms of the optimal values for the parameters A, B, and C of eq 5.

Conclusions

The HNHA experiment is a sensitive and simple experiment for obtaining H^N–H^α correlations in ^{15}N-labeled proteins. Although the HNHA experiment in principle is a variation of the COSY experiment,[43] resulting line shapes are in-phase and purely absorptive in all three dimensions. Excellent resolution in the ^{15}N dimension is obtained because of the relatively long duration of the ^{15}N constant-time evolution period.[44] Sensitivity of the experiment benefits from a number of factors. First, the duration of 2ζ is adjusted such as to maximize transfer from H^N to antiphase H^α magnetization and *vice versa*. In contrast, in a regular COSY experiment t_1 is incremented, resulting in low cross-peak signal obtained from short and from long durations of t_1. Second, dephasing and rephasing of magnetization takes place for H^N only, and unlike the regular COSY experiment, sensitivity does not suffer significantly from passive couplings between H^α and

(43) Aue, W. P.; Bartholdi, E.; Ernst, R. R. *J. Chem. Phys.* **1976**, *64*, 2229–2246.
(44) Madsen, J. C.; Sørensen, O. W. *J. Magn. Reson.* **1992**, *100*, 431–436.

H^β protons. Moreover, because signal is not attenuated during the ^{15}N evolution period, which overlaps with the H^N–H^α de- and rephasing periods, addition of the ^{15}N dimension causes minimal signal loss. Fourth, the transverse amide magnetization relaxes with the T_2 of the ^{15}N–H^N multiple quantum coherence during the periods, $2T$, preceding and following the t_2 evolution period. Because the transverse relaxation of the heteronuclear multiple quantum coherence is not affected by $J(0)$ spectral density terms containing the ^{15}N–H^N dipolar coupling,[45] the T_2 of the multiple quantum coherence is longer than that for the amide protons, reducing magnetization loss.

Measurement of the J coupling from the cross-peak to diagonal-peak ratios is a particularly simple operation, which compares favorably to interactive fitting procedures used for many other types of J coupling measurements. The fact that the J couplings, after a small (11%) and uniform correction for the effects of ^1H–^1H cross relaxation, show excellent agreement with J values predicted on the basis of the crystal structure indicates that the method yields quite accurate results. In SNase, J couplings as small as 3 Hz give rise to observable H^N–H^α cross peaks, making the experiment a useful alternative to the triple-resonance H(CA)-NH and HN(CA)H type experiments.[10,20-23] The HNHA experiment, however, has the added advantage of yielding the informative H^N–H^α coupling constant information.

Acknowledgment. We thank Frank Delaglio for writing the nonlinear least-squares fitting software used for intensity measurement of partly overlapping resonances, Dennis Torchia for encouragement and for the use of the SNase sample, Toshimaza Yamazaki for providing the stereospecific assignments of the glycine protons in SNase, and Rolf Tschudin for building the gradient pulse-shaping unit and amplifier. This work was supported by the AIDS Targeted Anti-Viral Program of the Office of the Director of the National Institutes of Health.

Supplementary Material Available: A table listing the ϕ angles and J values for SNase, and a product operator description of the HNHA correlation scheme (8 pages). Ordering information is given on any current masthead page.

(45) Bax, A.; Kay, L. E.; Sparks, S. W.; Torchia, D. A. *J. Am. Chem. Soc.* **1989**, *111*, 408–409.
(46) Shaka, A. J.; Keeler, J.; Frenkiel, T.; Freeman, R. *J. Magn. Reson.* **1983**, *52*, 334–338.